

Effect of Heat Treatment on the Microstructure and Mechanical Properties of Mg-3.4Y-3.6Sm-2.6Zn-0.8Zr Alloy

Liu Minghua, Wang Wenli, Zhang Mengqi, Qiu Yulong

Xi'an University of Architecture and Technology, Xi'an 710055, China

Abstract: The microstructure evolution and mechanical properties of Mg-3.4Y-3.6Sm-2.6Zn-0.8Zr (wt%) alloy after different heat treatments were investigated by differential thermal analysis (DSC), optical microscopy (OM), hardness test, X-ray diffraction (XRD), scanning electron microscopy (SEM), energy dispersive spectroscopy (EDS), and tensile test, and an optimum heat treatment system of solid-solution treatment at 500 °C for 15 h and aging treatment at 225 °C for 40 h was proposed. The results show that after the solution treatment at 500 °C for 15 h, the layer long period stacking ordered (LPSO) structure disappears, whereas the reticular (Mg,Zn)₃(Y,Sm) phases at the grain boundaries dissolve into granular phases, and the number of long strip phase Mg₁₂(Y,Sm)Zn increases at the same time. After the aging treatment, a large number of dispersed β' phases precipitate in the α-Mg grains, which is beneficial to the yield strength improvement of the alloy. The yield strength (YS), ultimate tensile strength (UTS) and elongation (EL) of the experimental alloy are 170.0 MPa, 260.8 MPa and 14.1%, respectively. The fracture mode of the as-cast alloy is intergranular brittle fracture, while that of the solution-treated alloy is cleavage fracture with a certain plastic deformation. The fracture mode of peak-aged alloy is mainly cleavage fracture.

Key words: magnesium alloy; heat treatment; microstructure; mechanical properties

Recently, magnesium alloys have attracted more and more attention as promising structural materials for replacing aluminum alloys in the automotive industry and aerospace technology^[1-4]. As the most common hexagonal-close packed (HCP) structural alloys, the deformation performance of cast magnesium alloys is poor. Therefore, it is essential to improve the mechanical properties of magnesium alloys by performing solid-solution treatment and aging treatment.

Due to the remarkable effect of purifying the melt, refining the grains and promoting the high-temperature mechanical properties, rare earth elements are the most widely added elements for increasing the strength and heat resistance of magnesium alloys^[5,6]. When two different subgroups (cerium subgroup and yttrium subgroup) of rare earth elements are added to magnesium alloys, the rare earth precipitation kinetics of each subgroup promotes the precipitation strengthening effect^[7]. In particular, Y which has the minimum density in the rare earth after Sc exhibits the best strengthening effect on the

magnesium alloys^[8]. The rare earth Sm which has the highest solid solubility of 5.8 wt% in the cerium subgroup shows the highest precipitation strengthening effect after undergoing a heat treatment^[9,10]. Indeed, precipitation hardening is the most effective mechanism for improving the high-temperature mechanical properties of magnesium alloys. Che et al^[11] found that the peak-aged Mg-4Sm-3Nd-Gd-Zn-Zr alloy exhibits excellent heat resistance with ultimate tensile properties of 213 MPa and elongation of 8.6 % at 300 °C.

In this study, the Mg-3.4Y-3.6Sm-2.6Zn-0.8Zr (wt%) alloy was prepared by metal die casting. The influence of the solution and aging treatment on microstructures and mechanical properties was investigated.

1 Experiment

The raw materials are pure Mg ingot (99.95 wt%), pure Zn ingot (99.98 wt%), Mg-Y master alloy (30.10 wt%), Mg-Sm master alloy (20.10 wt%) and Mg-Zr master alloy (34.50 wt%).

Received date: July 23, 2018

Foundation item: Science New Star Foundation of Shaanxi Province (2012KJXX-33); Science and Technology Project of Xi'an City (CXYJZKD003); Science and Technology Project of Yulin City

Corresponding author: Wang Wenli, Ph. D., Professor, School of Metallurgical Engineering, Xi'an University of Architecture and Technology, Xi'an 710055, P. R. China, Tel: 0086-29-82205569, E-mail: wangwl@nwpu.edu.cn

Copyright © 2019, Northwest Institute for Nonferrous Metal Research. Published by Science Press. All rights reserved.

The alloy was smelted in a pit-crucible resistance furnace, where a mixed gas (1 vol% SF₆+99 vol% CO₂) was introduced. The preheated magnesium ingot was added to the crucible at 750 °C. After the magnesium ingot was melted, pure Zn, Mg-Y and Mg-Sm master alloys were sequentially added. Then, when the temperature was increased to 780 °C, the Mg-Zr master alloy was added. When the temperature dropped to 750 °C, the refining agent C₂Cl₆ was added. The melt was cast into a steel mold, followed by water cooling. The heat treatment of the alloy was carried out in a muffle furnace. The heat-treated samples were immersed in a corundum crucible containing magnesia for heat insulation. These samples were incubated at 500 °C for 15 h and then rapidly quenched in hot water at 80~90°C. After the above operation, the samples were aged in air at 200, 225 and 250 °C for 5~75 h. Finally, the samples were air-cooled.

To determine the best solution-treatment temperature, the STA449F3 synchronous thermal analyser was used for thermal analysis of casting alloy. The heating rate was 10 °C/min, while the temperature changed from room temperature to 700 °C. Microstructures of different states of the alloy were examined via the OLYMPUS GX71 optical microscope (OM) and the JEOL JSM-6390A scanning electron microscope (SEM). Phases were identified via the D8 ADVANCE A25 X-ray diffraction (XRD) apparatus. The room-temperature tensile tests were conducted on the INSTRON8801 CNC tensile testing machine with a crosshead speed of 1 mm/min. Hardness was tested via the 401MVD semi-automatic micro Vickers hardness tester with the loading load of 200 gf and the loading time of 15 s.

2 Results

2.1 DSC analysis

Fig.1 shows the DSC curve of the as-cast Mg-3.4Y-3.6Sm-2.6Zn-0.8Zr alloy. Two endothermic peaks appear in the DSC curve. As shown in the left peak, the onset and peak temperatures of endothermic reaction were 502.7 and 510.1 °C, respectively, indicating that the melting of the eutectic phase is initiated at 502.7 °C. And the eutectic phase has a melting temperature in the range of 502.7~521.1 °C. As can be seen from the right peak, the onset and end temperatures are 615.5 and 640.4 °C, respectively, indicating that the solid-liquid temperature range of the alloy is 615.5~640.4 °C. To obtain the maximum supersaturated solid solubility, the solution-treatment temperature of magnesium alloys should be maintained lower than the melting temperature of the eutectic phase by 5°~10°. Therefore, the solution-treatment temperatures were selected to be 480, 500, 510 °C, and the solution-treatment time was selected within the range of 5~25 h.

2.2 Solid-solution treatment

Fig.2 shows the influence of the solution-treatment temperature and the solution-treatment time on the microstructure evolution of the selected alloys. With the increase of solu-

tion-treatment temperature, the layer long period stacking ordered (LPSO) structure gradually disappears, while the reticular phases at the grain boundaries dissolve into granular phases and the number of long strip phase increases at the same time. With the increase of solution-treatment time, grains grow up significantly. Some second phases still exist along the grain boundaries when the temperature is 480 °C, indicating that the temperature is too low for effective solution treatment. Compared with the microstructure of the alloy at 500 °C, a small number of grains are overheated at 510 °C, and the grains become coarse. In order to promote the full dissolution of the second phase into the α -Mg matrix without overheating and obvious grain growth, the solid-solution treatment at 500 °C for 15 h was chosen.

2.3 Age-hardening behavior

Fig.3 shows the age-hardening curves of the solid solution-treated alloys at 200, 225, and 250 °C for 5~75 h. As the aging temperature increases, the time to reach the aging peak decreases. When aged at 225 °C, the hardness of the alloy grows slowly in the initial stage (5~25 h) and then increases rapidly at 25~40 h. The highest hardness of 785.5 MPa was obtained when the sample was peak-aged at 225 °C for 40 h. After the aging time reached 40 h, the hardness declined slightly. At 250 °C, the alloy shows the weakest hardening response. Therefore, the best aging treatment is at 225 °C for 40 h.

3 Discussion

3.1 Phase analysis

Fig.4 shows the results of XRD of the alloys under different conditions. The phase components of the experimental alloys include α -Mg, (Mg,Zn)₃(Y,Sm), and Mg₁₂(Y,Sm)Zn. After the solution treatment was performed, the peak intensity of (Mg,Zn)₃(Y,Sm) decreased significantly, while the peak intensity of Mg₁₂(Y,Sm) Zn phase increased. As can be seen from Fig.4, the heat treatment process results in a solid phase transformation of the (Mg,Zn)₃(Y,Sm) and Mg₁₂(Y,Sm)Zn phases.

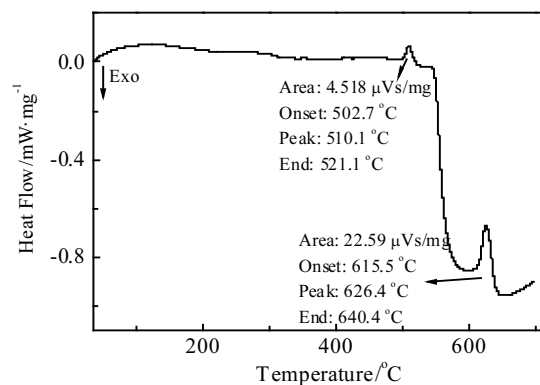


Fig.1 DSC curve of the as-cast Mg-3.4Y-3.6Sm-2.6Zn-0.8Zr alloy

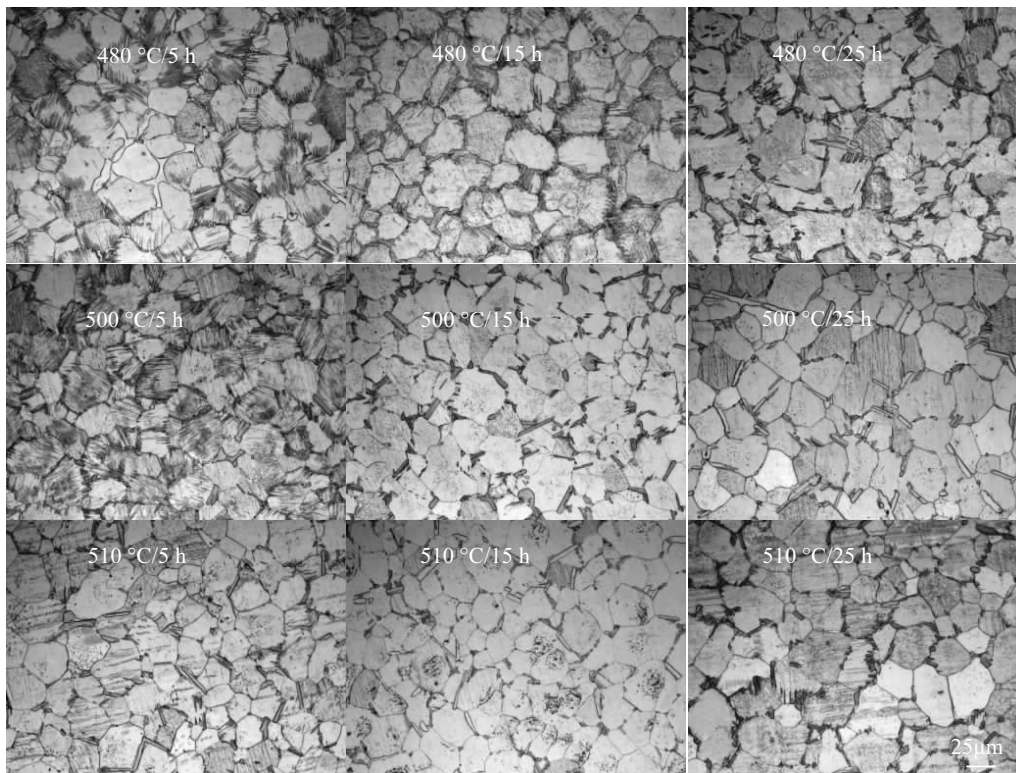


Fig.2 Optical microstructures of the Mg-3.4Y-3.6Sm-2.6Zn-0.8Zr alloy under different solution-treatment conditions

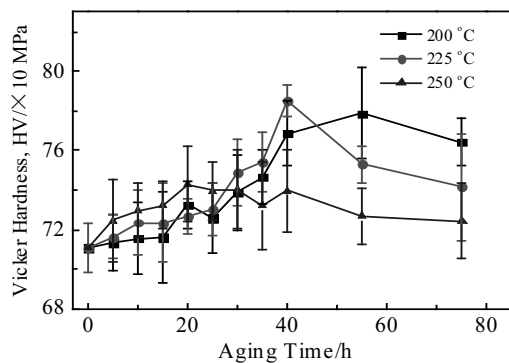


Fig.3 Age-hardening curves of the solid-solution-treated alloy

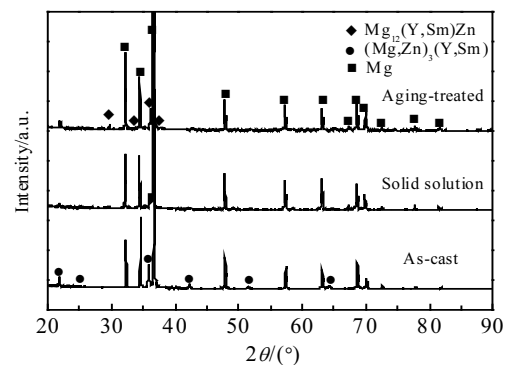


Fig.4 X-ray diffraction patterns of the alloys under different conditions

3.2 Microstructure

Fig.5a, 5c, and 5e show the microstructures of the alloys under different heat treatment conditions. In Fig.5a, the average grain size is about 23 μm , whereas the cast alloy is composed of α -Mg, long strip phase and reticular phase along the grain boundary. The LPSO structure diffuses from the grain boundaries to the inner grains. As shown in Fig.5c, after reaching the temperature of 500 $^{\circ}\text{C}$ and holding for 15 h, the LPSO structure disappears, while the $(\text{Mg,Zn})_3(\text{Y,Sm})$ phase along the grain boundaries changes from a reticular phase to a small particle. However, the number of the long strip phase $\text{Mg}_{12}(\text{Y,Sm})\text{Zn}$ increases at the grain boundaries. By the

aging treatment at 225 $^{\circ}\text{C}$ for 40 h, the small precipitated phases appear within the grains, which is the primary factor for improving the yield strength of the alloy, as illustrated in Fig.5e. After the heat treatment, only a small number of grains grow up, and the average grain size of the alloy is about 33 μm .

Fig.5b, 5d, and 5f show the SEM morphologies and corresponding EDS selected areas of the alloy under different heat treatment conditions. After solution treatment, the reticular phase gradually turns into a spherical phase without any change in composition, whereas the long strip phase increases signifi-

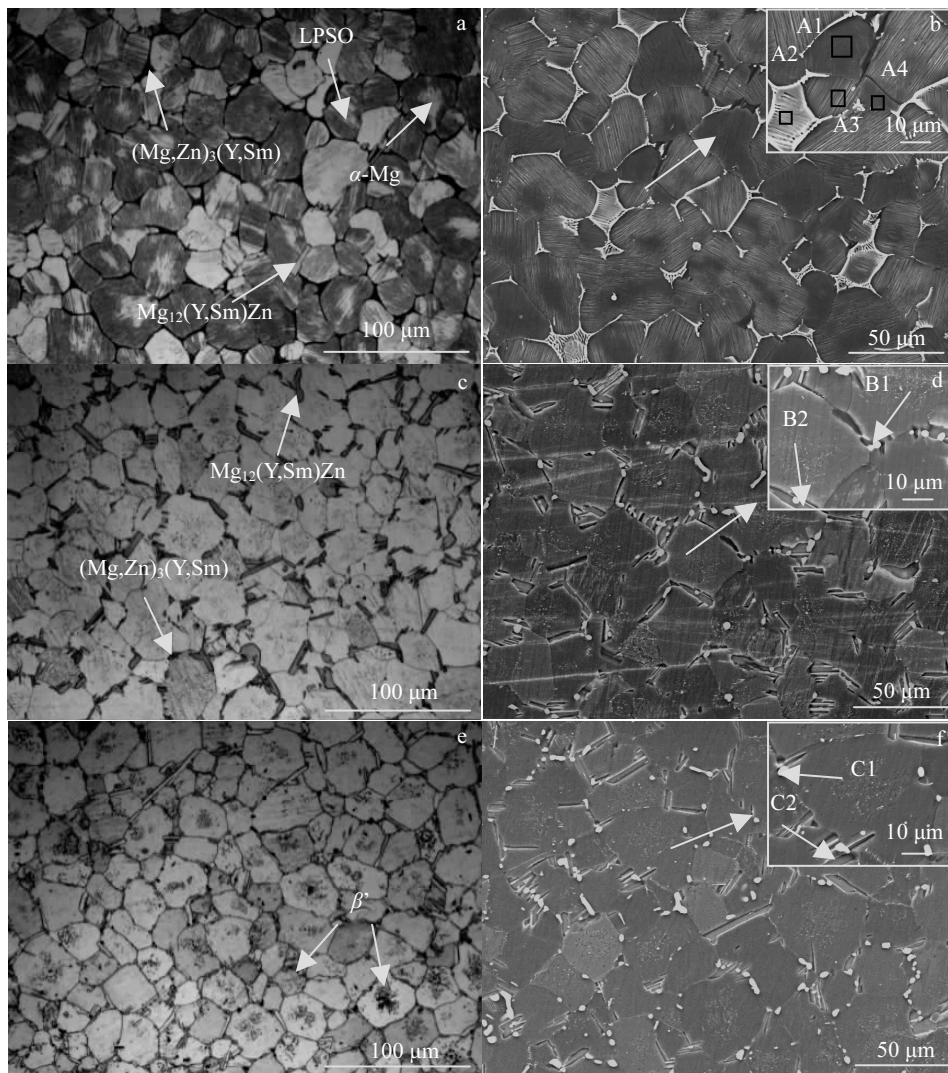


Fig.5 OM (a, c, e) and SEM (b, d, f) microstructures of the Mg-3.4Y-3.6Sm-2.6Zn-0.8Zr alloy: (a, b) as-cast, (c, d) 500 °C/15 h, and (e, f) 225 °C/40 h

Table 1 EDS analysis of the selected areas in Fig.5b, 5d and 5f (at%)

Element	A1	A2	A3	A4	B1	B2	C1	C2
Mg	98.22	54.71	97.24	87.59	52.53	85.66	52.27	91.45
Y	0.63	8.90	1.22	4.67	8.26	5.11	8.97	2.89
Sm	0.60	13.84	0.44	2.66	14.79	3.22	13.97	2.10
Zn	0.56	22.55	1.10	5.09	24.12	5.65	24.79	3.46

cantly. After the aging heat treatment, the dispersed second phase precipitates in the grain. Table 1 lists the EDS results for the microanalysis of the alloy displayed in Fig.5b, 5d, and 5f. The areas of A2, B1, and C1 have similar elemental components, and the atomic ratio (Mg+Zn):(Y+Sm) approaches 3:1, indicating that the phase of these areas is $(\text{Mg,Zn})_3(\text{Y,Sm})$, which is consistent with the XRD analysis. Similarly, the atomic ratio of $\text{Mg}:(\text{Y+Sm}):Zn$ of the long strip phase (A4, B2,

and C2) approaches 12:1:1, and it can be identified as the $\text{Mg}_{12}(\text{Y,Sm})Zn$ phase.

3.3 Mechanical properties

Fig.6 displays the typical stress-strain curves of the alloys. Compared with other cast magnesium alloys, the Mg-3.4Y-3.6Sm-2.6Zn-0.8Zr alloy exhibits excellent mechanical properties due to the fine-grain strengthening. The yield strength (YS), ultimate tensile strength (UTS), and elon-

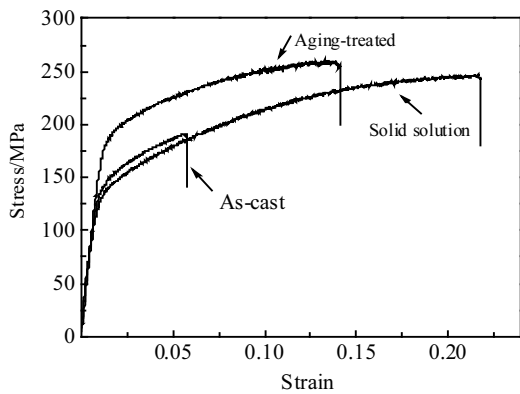


Fig.6 Stress-strain curves of the as-cast and heat treated alloys

gation (EL) are 122.3 MPa, 191.5 MPa, and 5.7%, respectively. After the solution treatment at 500 °C for 15 h, the UTS and EL increase significantly due to the solid-solution strengthening. Moreover, the coarse $(\text{Mg,Zn})_3(\text{Y,Sm})$ phases at the grain boundaries are transformed into small spherical particles, which substantially enhances the elongation of the experimental alloy. The YS, UTS, and EL values of the solution-treated alloy are 119.4 MPa, 245.3 MPa, and 21.4%, re-

spectively. Finally, after the aging treatment at 225 °C for 40 h, the finely dispersed second phase can significantly improve the yield strength. The alloy shows the optimal mechanical properties of 170.0 MPa in YS, 260.8 MPa in UTS, and 14.1% in EL.

The SEM morphologies of the fracture surfaces of the alloy under different conditions are shown in Fig.7. The fracture surface of the as-cast alloy consists of cracked eutectic phases and cleavage planes. The fracture mode is intergranular brittle fracture and the fracture mainly occurs at the grain boundaries where eutectic particles exist. The fracture surface of the solution-treated alloy consists of cleavage planes and secondary phase particles. There are some dimples with different depths and obvious tear ridges on the fracture surface, indicating that plastic deformation occurs before fracture failure. The fracture mode of the solution-treated alloy is cleavage fracture with a certain plastic deformation, and the plasticity of the alloy is greatly improved. The elongation of the solution-treated alloy is 21.4%. Compared with the solution-treated alloy, the number of dimples and tear ridges on the fracture surface of peak-aged alloy decreases, and the elongation of peak-aged alloys decreases to 14.1%. The fracture mode of peak-aged alloy is mainly cleavage fracture.

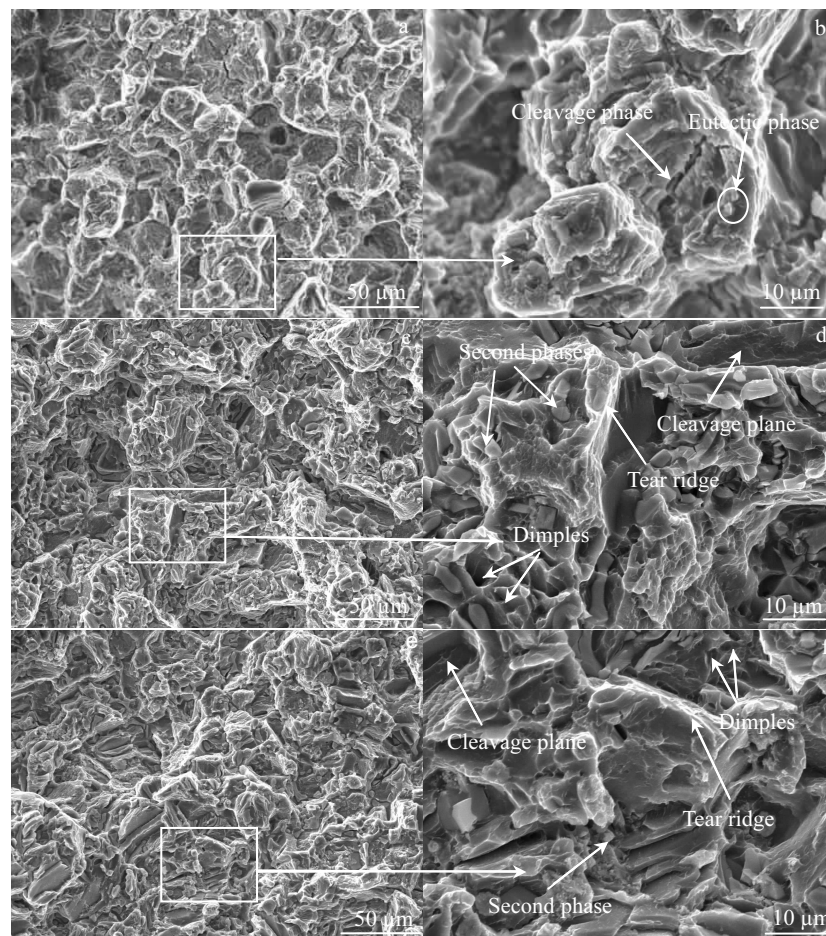


Fig.7 SEM morphologies of fracture surfaces of the alloy under different conditions: (a, b) as-cast, (c, d) solution-treated, and (e, f) peak-aged

4 Conclusions

1) The optimal heat treatment process is a combination of solid-solution treatment at 500 °C for 15 h and aging treatment at 225 °C for 40 h.

2) The as-cast alloy is composed of α -Mg, $(\text{Mg,Zn})_3(\text{Y,Sm})$ and $\text{Mg}_{12}(\text{Y,Sm})\text{Zn}$. After the solution treatment, the layer LPSO structure disappears, whereas the $(\text{Mg,Zn})_3(\text{Y,Sm})$ dissolves from the reticular phase into a spherical phase, and the number of long strip phase $\text{Mg}_{12}(\text{Y,Sm})\text{Zn}$ increases at the same time.

3) After the aging treatment, a large amount of dispersed $(\text{Mg,Zn})_3(\text{Y,Sm})$ phases precipitate in the α -Mg grains, and an excellent combination of strength and ductility is obtained, which is 170.0 MPa in YS, 260.8 MPa in UTS, and 14.1% in EL.

4) The micro-cracks in the as-cast alloy can be identified in the cracked second phases. The fracture mode of the as-cast alloy is intergranular brittle fracture. The fracture mode of the solution-treated alloy is cleavage fracture with a certain plastic deformation. The fracture mode of peak-aged alloy is mainly cleavage fracture.

References

- 1 Mordike B L, Ebert T. *Materials Science & Engineering A*[J], 2001, 302(1): 37
- 2 Sun Jing, Zhang Dingfei, Tang Tian et al. *Rare Metal Materials & Engineering*[J], 2017, 46(7): 1768
- 3 Joost W J, Krajewski P E. *Scripta Materialia*[J], 2017, 128: 107
- 4 Zhang Daidong, Hao Xiaowei, Fang Daqing et al. *Rare Metal Materials & Engineering*[J], 2016, 45(9): 2208
- 5 Liang Chenghao, Wang Shusen, Huang Naibao et al. *Rare Metal Materials and Engineering*[J], 2015, 44(3): 521
- 6 Guan K, Yang Q, Bu F et al. *Materials Science & Engineering A*[J], 2017, 703: 97
- 7 Rokhlin L L, Dobatkina T V, Nikitina N I. *Materials Science Forum*[J], 2003, 419: 291
- 8 Liu X, Shan D, Song Y et al. *Journal of Magnesium & Alloys*[J], 2017, 5: 26
- 9 Zheng J, Zhou W, Chen B. *Materials Science & Engineering A*[J], 2016, 669: 304
- 10 Zheng J, Wang Q, Jin Z et al. *Materials Science & Engineering A*[J], 2010, 527(7-8): 1677
- 11 Che C J, Cheng L R, Tong L B et al. *Journal of Alloys & Compounds*[J], 2017, 706: 526

热处理对 Mg-3.4Y-3.6Sm-2.6Zn-0.8Zr 合金组织和性能的影响

刘明华, 王文礼, 张梦奇, 邱玉龙
(西安建筑科技大学, 陕西 西安 710055)

摘要: 采用差热分析(DSC)、光学显微镜(OM)、硬度测试、X射线衍射(XRD)、扫描电子显微镜(SEM)、能量色散谱(EDS)及拉伸测试等手段研究了 Mg-3.4Y-3.6Sm-2.6Zn-0.8Zr(质量分数, %)合金经过不同热处理方式后的组织演变及力学性能。提出了 500 °C 固溶处理 15 h、225 °C 时效处理 40 h 的最佳热处理制度。500 °C 固溶处理 15 h 后, 层状长周期堆积有序(LPSO)结构消失, 晶界处的 $(\text{Mg,Zn})_3(\text{Y,Sm})$ 从网状相溶解成颗粒状, 长条状 $\text{Mg}_{12}(\text{Y,Sm})\text{Zn}$ 相的数量增加。时效处理后, 大量弥散 β' 相析出到 α -Mg 晶粒中, 有利于提高合金的屈服强度。试验合金的屈服强度(YS)、抗拉强度(UTS)和延伸率(EL)分别为 170.0 MPa、260.8 MPa 和 14.1%。铸态合金的断裂方式为沿晶脆性断裂, 固溶处理合金的断裂模式是具有一定塑性变形的解理断裂, 峰值时效合金的断裂模式以解理断裂为主。

关键词: 镁合金; 热处理; 显微组织; 力学性能

作者简介: 刘明华, 男, 1976 年生, 讲师, 西安建筑科技大学, 陕西 西安 710055, 电话: 029-82205569, E-mail: 513629738@qq.com